Indian Journal of Pure & Applied Physics
Vol. 55, January 2017, pp. 19-24

Deposition of alumina films by inverted cylindrical magnetron sputtering assisted by optical emission spectroscopy

Atul Khanna[a]* & Deepak G Bhat[b]**

[a]Department of Physics, Guru Nanak Dev University, Amritsar 143 005, India
[b]Department of Mechanical Engineering, University of Arkansas, AR 72701, USA

Received 13 July 2015; revised 19 October 2016; accepted 4 November 2016

Alumina coatings have been deposited on glass substrates by reactive ac (41 kHz) magnetron sputtering of two hollow aluminum targets in argon-oxygen plasma at 5 kW sputtering power in the poisoned mode and in the unstable region of hysteresis loop of reactive sputtering. The poisoned mode produces nanocrystalline films of γ and δ alumina at a low deposition rate of 0.06 nm·s^{-1}. Amorphous alumina films have been grown at a higher deposition rate of 0.2 nm·s^{-1} with the aid of optical emission spectroscopy in which the feedback signal of Al emission spectral line at 396 nm monitored Al concentration in the plasma discharge and accomplished the controlled oxidation of targets during reactive sputtering. Dynamic secondary ion mass spectroscopy studies confirm that alumina films grown in the unstable region of the hysteresis loop of reactive sputtering are highly stoichiometric and of uniform composition with film thickness. Our study demonstrates the successful coupling of optical emission spectroscopy with hollow cylindrical magnetrons for deposition of alumina films.

Keywords: Alumina films, Reactive sputtering, Inverted cylindrical magnetrons, Optical emission spectroscopy, XRD, SIMS

1 Introduction

Alumina films are of great interest because of their applications such as transparent, hard and corrosion resistant protective top layers. Crystalline and amorphous alumina films have been prepared by variety of techniques such as electron beam evaporation[1,2], RF sputtering[3,4], pulsed DC sputtering[5-7], mid frequency AC sputtering[8], pulsed laser deposition[9-12], chemical vapour deposition[13-15] and plasma spraying[16]. Mid-frequency ac (41 kHz) reactive unbalanced magnetron sputtering offers unique advantages of high ion bombardment during thin film growth. Due to the unique geometry of hollow cylindrical magnetrons, growing films are subjected to significant ion bombardment and the technique produces crystalline alumina films at moderate sputtering power densities of 2 to 3 W cm^{-2} without any deliberate substrate heating[8].

In the poisoned mode of reactive sputtering, high concentration of oxygen gas is used and metal targets are covered with thin layers of aluminum oxide; this produces crystalline alumina films but at low growth rate. Several methods have been proposed for the enhancement of alumina deposition rate: (i) separation of reactive gas from target by using baffles[17,18] (ii) hollow cathode substrate holders[19,20] (iii) feedback signal from target current or voltage[21] and (iv) optical emission spectroscopy (OES)[22,23]. Alumina films grown by RF sputtering and electron beam evaporation, without high temperature substrate heating are usually amorphous[1-4]. Although α-alumina (corundum) is the most desirable crystalline phase of aluminum oxide, amorphous alumina coatings are also of significant interest as they find application as corrosion resistant top layers; amorphous alumina is also a biocompatible and bioactive material[24]. Amorphous anodic alumina is used as template for growing nanowires of metals and oxides[25]. Amorphous alumina films are used a dielectric layers in microelectronic devices, since these have an advantage over crystalline films that the thermal conductivity increases with increase in temperature and these are more efficient for the dissipation of heat in microelectronic circuits[26].

In the present study we have investigated the growth and characterization of alumina films in the ICM-10 coating unit (ISOFLUX Inc. Rochester, NY, USA) under two conditions: (i) deposition in the poisoned mode of Al targets and (ii) deposition in the

*Corresponding author (E-mail: atul.phy@gndu.ac.in)
**Deceased

unstable region of hysteresis loop of reactive sputtering assisted by OES, which regulates the oxidation, i.e., poisoning of Al targets. During the two runs sputtering power was kept constant at 5 kW. The objective of this study is to demonstrate the successful coupling of OES with hollow cylindrical magnetrons for alumina film deposition in the unstable region of hysteresis loop of reactive sputtering.

2 Experimental

2.1 Alumina deposition in the poisoned mode

The schematic of the sputtering system ICM-10 is shown in Fig. 1. The coating unit consists of two hollow cylindrical (ring) targets of Al (99.5 % purity, 33 cm diameter and 9.8 cm height) and an advanced energy AC power supply (Model PE II) operated at a mid-frequency of 41 kHz and constant power of 5 kW. The first run was performed in the poisoned mode of targets using constant Ar and O_2 gas flow of 88 SCCM and 48 SCCM, respectively, shown in Table 1. The O_2 flow rate was high enough to cover the targets surfaces with thin layer of aluminum oxide. This reduces the sputtering yield from the targets causing a low thin film growth rate, but the film samples are close to the required stoichiometry.

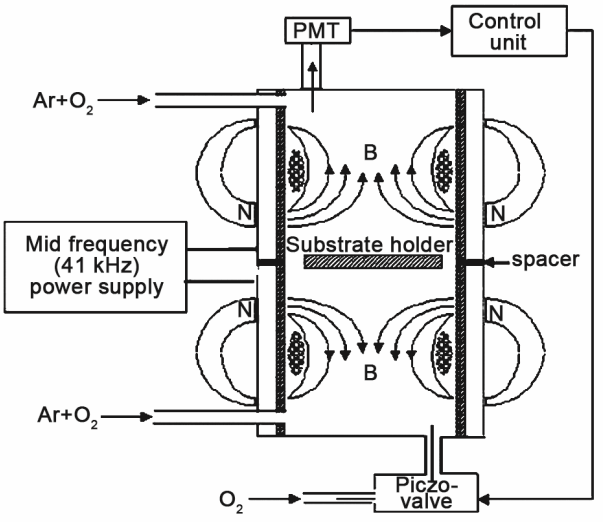

Fig. 1 – Schematic of mid frequency AC magnetron sputtering unit (ICM-10) with optical emission spectroscopy system to control hysteresis effects in target poisoning

This is commonly known as the poisoned mode of the targets. During both runs several pieces (5 to 6) of ultrasonically cleaned, glass substrates were kept on a horizontal steel plate enclosed by the two rings of Al. The chamber was evacuated to a base vacuum in the range of 1.2 to 3×10^{-4} Pa with a turbo molecular pump and then Ar and O_2 gases (99.99 % purity) were admitted and power supply was switched on to create the plasma discharge. The poisoned mode run was carried out for 4 h. No deliberate substrate heating was provided during deposition and the substrates were kept at a floating potential.

2.2 Alumina deposition in the unstable region of hysteresis by optical emission spectroscopy

During the run 2, alumina deposition was carried out in the unstable region of reactive sputtering hysteresis loop by using the feedback signal of optical emission spectroscopy (OES). In this run besides introducing mixture of Ar and O_2 gases through two orifices at the top and bottom of the chamber (Fig. 1), oxygen gas was also simultaneously introduced into the chamber with a fast response time piezo-electric valve (Model PEV-1, Key High Vacuum Products Ltd. USA). The opening and closing of the piezo-electric valve was regulated by electrical pulses from an electronic control unit (Gas Clutch provided by Corona Vacuum Coaters Inc., Canada). This electronic control unit received an input signal from the photomultiplier tube (PMT) (Hamamatsu H5783-01) which measured the intensity of light emitted at 396 nm by excited Al atoms in plasma discharge. Light of only this wavelength was allowed to fall on the cathode of the photomultiplier tube (PMT) by an optical filter (Fig. 1). At constant target power and gas flow rates, the intensity of light emitted at 396 nm is proportional to the concentration of sputtered Al atoms in the plasma. Since sputtering yields from metallic targets are significantly higher than from oxidized (i.e. poisoned) targets[26], a higher PMT signal implies lower poisoning of the targets by O_2 gas.

The operation of the electronic control unit (Gas Clutch) was performed through special computer software (Dual Exe program provided as a part of Gas Clutch) which allowed us to do reactive sputtering at

Table 1– Parameters used for the deposition of alumina films in runs 1 and 2.

Deposition run no.	Chamber Pressure (Pa)	Ar (SCCM)	O_2 (SCCM)	Substrate	Mode of deposition	Deposition time (s)
1	0.33	88	48	Glass	Poisoned	14400
2	0.19 to 0.23	75	5	Glass	Unstable region of the hysteresis loop	6200

different levels of the target poisoning. The extent of poisoning was measured and regulated by "PMT signal set point" value in the computer program. Higher the set point, lesser O_2 was delivered into the chamber (through the piezo-electric valve), as a result the targets were poisoned to a smaller extent. For example a set point of 0.9 allowed only enough O_2 into the deposition chamber to provide a 10 % reduction in the Al signal, similarly a set point of 0.4 causes sufficient O_2 being introduced into the chamber to provide a 60% reduction in the metal signal, indicating relatively greater poisoning of the targets. A study of hysteresis effects on target voltage and current as a function of O_2 gas flow rate during reactive sputtering of Al in the ICM-10 system found that Ar flow rate of 75 SCCM required O_2 flow rate of ~40 SCCM for completely poisoning the dual targets of ICM-10 system[8] at a discharge power of 5 kW.

Alumina deposition run assisted by OES was performed with a set point value of 0.157 in the dual exe computer program at a constant sputtering power of 5 kW and Ar and O_2 flow rates of 75 SCCM and 5 SCCM, respectively (Table 1). This particular set point value, along with Ar and O_2 flow rates of 75 SCCM and 5 SCCM, respectively accomplished the deposition of transparent, stoichiometric and highly insulating alumina films. Before each alumina run, Al targets were cleaned by sputtering in pure Ar discharge at 6.5 kW for one hour. At the end of this cleaning run, the PMT signal at 396 nm was normalized to 1. This was followed by reactive sputtering in Ar-O_2 plasma in the unstable region of hysteresis. The deposition parameters during two runs are summarized in Table 1. A shutter enabled the physical isolation of the substrates from the targets. The oxidation of the targets did not occur immediately but typically about 10 to 15 s after the start of deposition recipe, during this time if the substrates were not covered, it resulted in the coating of Al pre-layer on the substrates, the deposition of Al pre-layer on the substrates was avoided by using the shutter between the targets and substrates. Deposition was carried out simultaneously on several samples to check the homogeneity of structural and optical properties of films.

2.3 Film thickness

Thicknesses of alumina films on glass substrates were measured by studying the interference effects in UV-visible transmission spectra. The spectra were measured on Shimadzu double-beam spectrophotometer (Model 2010 PC). By noting the wavelength difference (λ_2-λ_1) between two successive interference minima and using the reported refractive index value of n = 1.76 and 1.65 for crystalline and amorphous alumina respectively[1,12] film thickness, t, were calculated by the following relationship[27-29]:

$$t = \frac{\lambda_1 \lambda_2}{2n(\lambda_2 - \lambda_1)} \quad \ldots (1)$$

2.4 X-ray diffraction

X-ray diffraction studies were carried out on alumina samples using Cu K_α x-rays (λ=1.54056 Å) on a powder diffractometer (Philips Model PW 1830). The X-ray tube was operated at 45 kV and 40 mA. The measurements were performed in grazing incidence X-ray diffraction (GIXRD) configuration by keeping the incidence angle fixed at 2.5° and scanning the proportional counter detector in the 2θ range of 10° to 100°.

2.5 Dynamic secondary ion mass spectrometry (SIMS)

To examine the uniformity of composition of films grown in the unstable region of hysteresis loop, SIMS studies were performed on one sample from run 2 using sapphire as a standard on the CAMECA-IMS-4F system. Films were top coated with a Au layer of thickness of about 50 Å and an electron flood gun was used during analysis to compensate for sample charging effects. Films surface were not sputter cleaned before recording the SIMS data; and no effort was made to protect the samples from atmospheric vapors after taking them out of the deposition chamber. The composition analysis was performed with 10 kV Cs^+ primary beam bombardment and by monitoring their positive secondary ions. The secondary ions were extracted from a 30 μm diameter circular region centered in the rastered area of the film. The rastered area was about 150 μm × 150 μm. Thin film depth was calibrated by measuring the depth of the sputtered crater using a Tencor Alpha Step 200 stylus profilometer.

3 Results and Discussion

3.1 Film thickness and deposition rate

Alumina films prepared during runs 1 and 2 were highly insulating and transparent in the UV visible range and showed interference effects when examined visually, and had excellent adhesion with glass substrates.

Figure 2 shows the UV-visible transmittance spectra of several films deposited in the poisoned

mode (run 1) and in the unstable region of hysteresis loop (run 2). The average thickness of crystalline films on glass substrates during poisoned mode (run 1) was 895 ± 30 nm, while thickness of amorphous films grown by run 2 was 1160 ± 70 nm. Film deposition rates in the poisoned mode and in the unstable region of hysteresis loop were 0.06 nm·s^{-1} and 0.20 nm·s^{-1}, respectively.

Alumina films grown by RF sputtering are usually found to be amorphous and one study reported[4] a deposition rate of 0.2 to 0.5 nm·s^{-1} depending upon the inter-electrode distance at a target power density of 6.4 W cm^{-2}. Electron beam evaporation usually forms amorphous alumina films; Proost and Spaepen[2] deposited stoichiometric amorphous alumina films at an average rate of 0.3 nm·s^{-1} by electron beam evaporation at *in-situ* substrate temperature of 600 °C. Electron beam evaporation has a disadvantage that it sometimes produces oxygen deficient films that have poor transparency in the UV visible region[1]. Schneider *et al.*[30] deposited amorphous alumina films by reactive pulsed DC magnetron sputtering at rates of 0.38-0.78 nm·s^{-1} by regulating the oxygen partial pressure in the coating unit at a chamber pressure of 0.67 Pa. Jones and Logan[19] achieved very high alumina deposition rate of 3.66 nm·s^{-1} by reactive sputtering at high pressure of 6.6-9.3 Pa. The primary factor that determines the deposition rate of films by sputtering is the power density.

It may be noted that the chamber pressure during run 2 was not constant but oscillated from 0.19 to 0.22 Pa (Table 1). This was because O_2 flow into the chamber via piezo valve varied with time as the target oscillated between metallic and oxidized states.

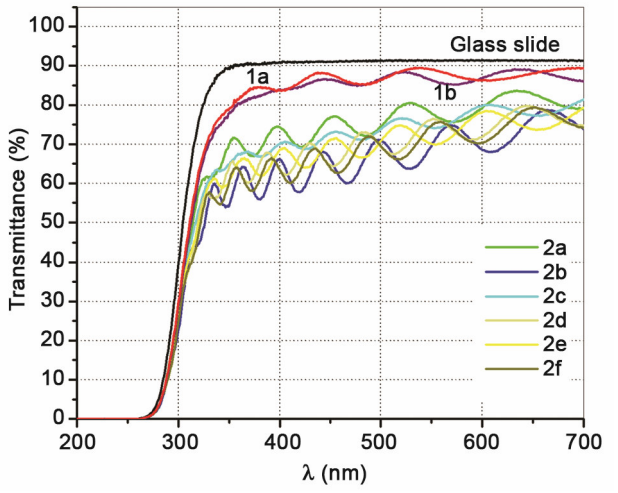

Fig. 2 – Interference effects in the UV-visible transmission spectra of alumina films grown during runs 1 and 2

3.2 Structure

An XRD pattern of one crystalline film on glass substrate prepared in the poisoned mode of Al targets (run 1) is shown in Fig. 3. Two characteristic broad peaks centered at 45.9° and 67.1° were detected in the samples grown during run 1. These two peaks match with γ and δ alumina phases[31,32] and could be due to the superposition of peaks due to both γ and δ phases. Two other weak peaks were detected at 37.7° and 61.0° which also matched with γ and δ phases.

Deposition run 2 produced amorphous alumina films (Fig. 3). The use of feedback signal from OES prevented the complete oxidation of metal targets in Ar-O_2 plasma and allowed the deposition in the unstable region of hysteresis loop of reactive sputtering at a faster rate (0.20 nm·s^{-1}), however films were not crystalline (Fig. 4).

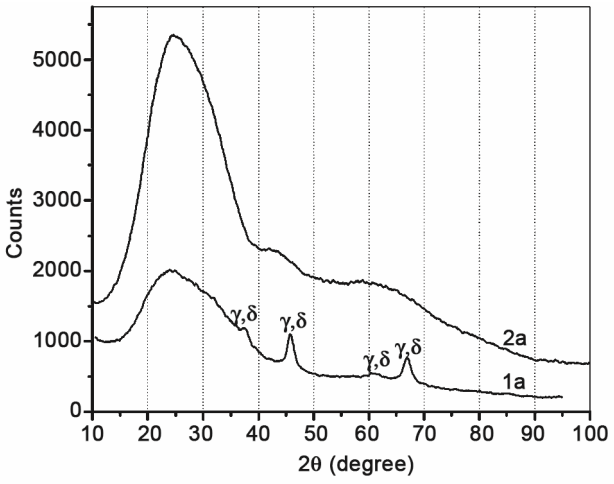

Fig. 3 – GIXRD patterns of alumina films on glass substrates grown during runs 1 and 2.

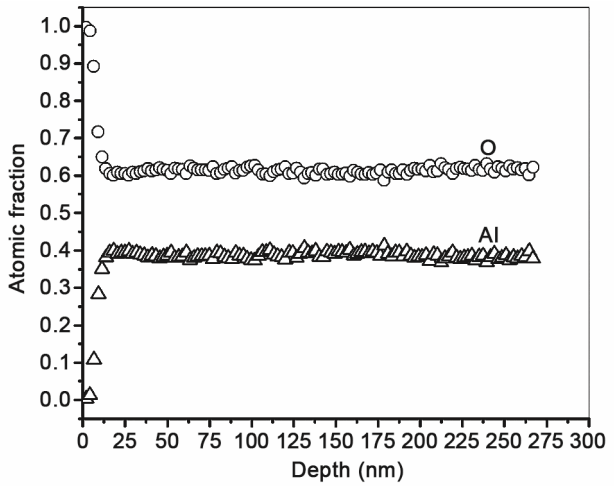

Fig. 4 – O and Al atomic ratio in amorphous alumina films as a function of thickness

The amorphous nature of films is due to two factors: higher growth rate and lower substrate temperature due to incomplete poisoning of the targets. The poisoned mode of reactive sputtering causes high secondary electron emission (SEE) from the targets[33] these electrons are picked up by oxygen species in the plasma, negative oxygen ions in turn bombard the substrate holder plate and heat it. The electron and negative ion bombardment raises the temperature to about 350 °C at sputtering power of 5 kW although the substrates were not heated deliberately during deposition[34].

The use of Gas Clutch enhances the deposition rate by preventing the complete poisoning (oxidation) of targets, but it also lowers SEE and hence the negative ion bombardment of the substrate holder. This lowers the substrate temperature and deteriorates film crystallinity.

3.3 Composition

The composition and uniformity of films grown by OES were studied by dynamic SIMS. These analysis showed that films were highly stoichiometric and contained 40 atomic % Al and 60 atomic % O (Fig. 4). Using reported density of 3.3 g cm^{-3} for amorphous alumina[35,36] Al and O concentration were calculated to be 4×10^{22} cm^{-3} and 6×10^{22} cm^{-3}, respectively. The top layers of the film (up to ~20 nm) contained excess of oxygen and hydrogen impurities probably due to water molecules adsorbed from the atmosphere. Small argon impurities were also present in the film due to use of argon during sputtering deposition (Fig. 5). At depths more than 50 nm, H concentration was 1.6×10^{20} cm^{-3} and Ar concentration was 4.9×10^{19} cm^{-3}. Therefore the hydrogen impurity concentration was very small ~ 0.1 atomic % in the amorphous alumina film.

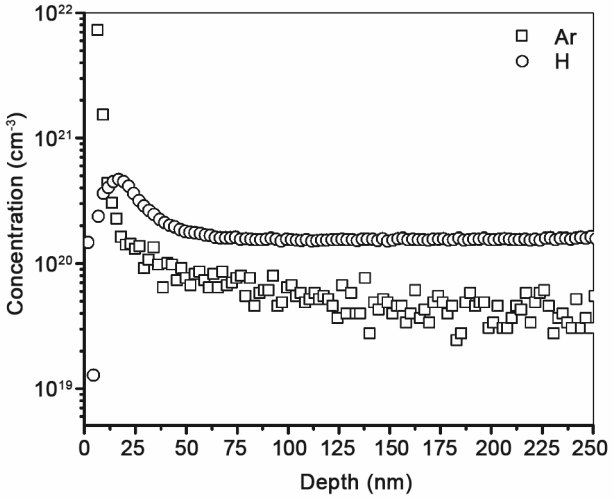

Fig. 5 – Hydrogen and argon impurity concentration in amorphous alumina films prepared by reactive sputtering assisted by OES

Depth profiling studies confirmed that composition of alumina film was uniform over a depth of at least 260 nm. Therefore highly stable deposition of alumina was achieved in the unstable region of hysteresis loop of reactive sputtering with the assistance of feedback signal from OES.

4 Conclusions

Crystalline and amorphous alumina films were prepared by reactive inverted cylindrical magnetron sputtering using mid frequency ac power supply in the novel geometry of dual hollow cylindrical targets. Amorphous alumina deposition was carried at a rate faster than that normally achieved by sputtering techniques at target power density of 2.4 Wcm^{-2} and was comparable to the growth rates usually reported with electron beam evaporation. Higher deposition rate was achieved by using optical emission spectroscopy that monitored Al concentration in the plasma and prevented the complete oxidation of metal targets. SIMS analysis showed that bulk composition of films was fairly uniform, although top layers (up to 20 nm) contained higher concentration of oxygen concentration probably due to water molecules adsorbed from the atmosphere post-deposition. It was concluded that optical emission spectroscopy (OES) is a reliable technique for growing uniform alumina films by regulating the hysteresis effects in reactive sputtering. OES along with *in-situ* substrate heating can produce crystalline alumina coatings at a higher deposition rates and at moderate sputtering power densities of 2 to 3 Wcm^{-2}.

Acknowledgement

Authors are thankful to Mr Mark Romach and Dr David Glocker, ISOFLUX INC., NY, USA and Prof Robert R Parsons, University of British Columbia, Canada for providing valuable guidance during the time this work was done at the University of Arkansas, Fayetteville, AR, USA. And Dr Jack Sheng, Qspec Technology, Sunnyvale, CA, USA is thanked for SIMS analysis on the samples. Arkansas Analytical Laboratory, University of Arkansas is acknowledged for providing the facility of XRD. This research was funded by National Science Foundation (NSF) under the NSF GOALI project grant # DMI-00400167 awarded to Prof Deepak G Bhat (deceased).

References

1 Nayar P, Khanna A, Kabiraj D, Abhilash S R, Beake B D, Losset Y & Chen B, *Thin Solid Films*, 568 (2014) 19.
2 Proost J & Spaepen F, *J Appl Phys*, 91 (2002) 204.
3 Thornton J A & Chin J, *Ceram Bull*, 56 (1977) 504.
4 Ramos F & Vieira M T, *Mater Manuf Process*, 7 (1992) 251.
5 Zywitzki O, Hoetzsch G, Fietzke F & Goedicke K, *Surf Coat Technol*, 82 (1996) 169.
6 Schneider J M, Sproul W D & Matthews A, *Surf Coat Technol*, 98 (1998) 1473.
7 Kohara T, Tamagaki H, Ikari Y & Fujii H, *Surf Coat Technol*, 185 (2004) 166.
8 A Khanna & D G Bhat, *Surf Coat Technol*, 201 (2006) 168.
9 Pillonnet A, Garapon C, Champeaux C, Bovier C, Brenier R, Jaffrezic H & Mugnier J, *Appl Phys A*, 69 (1999) 735.
10 Cibert C, Hidalgo H, Champeaux C, Tristant P, Tixier C, Desmaison J & Catherinot A, *Thin Solid Films*, 516 (2008) 1290
11 Ferre F G, Bertarelli E, Chiodoni A, Carnelli D, Gastaldi D, Vena P, Beghi M G & Fonzo F D, *Acta Mater*, 61 (2013) 2662
12 Nayar P & Khanna A, *Euro Phys J Appl Phys*, 64 (2013) 10301.
13 Ruppi S & Larsson A, *Thin Solid Films*, 388 (2001) 50.
14 Ruppi S, *Thin Solid Films*, 23 (2005) 306.
15 Etchepare P L, Vergnes H, Samélor D, Sadowski D, Caussat B & Vahlas C, *Surf Coat Technol*, 275 (2015) 167.
16 Jordan E H, Gell M, Sohn Y H, Goberman D, Shaw L, Jiang S, Wang M, Xiao T D, Wang Y & Strutt P, *Mater Sci Eng A*, 301 (2001) 80.
17 Scherer M & Wirz P, *Thin Solid Films*, 119 (1984) 203.
18 Pang T M, Scherer M, Heinz B, Williams C & Chaput G N, *J Vac Sci Technol A*, 7 (1989) 1254.
19 Jones F & Logan J, *J Vac Sci Technol A*, 7 (1989) 1240.
20 Pradhan A A, Shah S I & Unruh K M, *Rev Sci Instrum*, 73 (2002) 3841.
21 Lindberg V W, Woodard A R & Glocker D A, *Surf Coat Technol*, 484 (2000) 133.
22 Schütze A & Quinto D T, Surf Coat Technol, 162 (2003) 174
23 Bobzin K, Lugscheider E, Maes M & Piñero C, *Thin Solid Films*, 494 (2006) 255.
24 Naji A & Marie-Françoise Harmand, *Biomaterials*, 12 (1991) 690.
25 Bhushan B, *Handbook of nanotechnology*, (Springer Verlag, Berlin Heidellberg), 2004.
26 Stark I, Stordeur M & Syrowatka F, *Thin Solid Films*, 226 (1993) 185.
27 Heavens O S, *Optical properties of thin solid films*, (Dover Publications, New York), 1965.
28 Manifacier J C, Gasiot J & Fillard J P, *J Phys E*, 9 (1976) 1002.
29 Swanepoel R, *J Phys E Sci Instrum*, 16, (1983) 1214.
30 Schneider J M, Sproul W D, Chia R W J, Wong M S & Matthews A, *Surf Coat Technol*, 96 (1997) 262.
31 ICDD, *Powder Diffraction File* # 10-0425, Newtown Square PA, USA.
32 ICDD, *Powder Diffraction File* # 46-1131, Newtown Square PA, USA.
33 Stirling A J & Westwood W D, *Thin Solid Films*, 7 (1971) 1.
34 Cloud A N, Aryasomayajula A, Bhat D G & Gordon M H, *Surf Coat Technol*, 202 (2008) 1564.
35 Gitzen W H, *Alumina as a ceramic material*, (American Ceramic Society, Columbus), 1970.
36 Wefers K & Misra C, *Oxides and hydroxides of aluminum*, ALCOA Technical Paper No 19, ALCOA Laboratories, 1987.